VOL. 17, NO. 4 J. AIRCRAFT APRIL 1980

ARTICLE NO. 80-4027

C 80-035

Flutter Analysis of a NACA 64A006 Airfoil in Small Disturbance Transonic Flow

20009
20018
30001

T.Y. Yang,* P. Guruswamy,† and Alfred G. Striz†
Purdue University, West Lafayette, Ind.
and
James J. Olsen‡
Air Force Wright Aeronautical Laboratories, Wright-Patterson AFB, Ohio

Flutter analyses are performed for a NACA 64A006 airfoil pitching and plunging in small-disturbance, unsteady transonic flow. Aerodynamic coefficients are obtained for $M_\infty = 0.7, 0.8, 0.85, 0.8625$, and 0.87, and for various values of low reduced frequencies. Two computer codes are used: 1) STRANS2 and UTRANS2 based upon the relaxation method and 2) LTRAN2 based upon the time-integration (indicial) method. Flutter results are presented as plots of flutter speed and corresponding reduced frequency vs one of the four parameters: airfoil/air mass density ratio, position of mass center, position of elastic axis, and freestream Mach number. In each figure, several sets of curves for different values of plunge/pitch frequency ratios are shown. The two sets of results based upon the two separate computer codes are, in general, in good agreement. For a special flutter analysis of a flat plate at $M_\infty = 0.7$, the present methods agree well with the linear flat plate theory. The effect of each parameter on the trend of each curve of flutter speed is discussed in detail. The examples demonstrate the dip phenomenon of the curves for flutter speed in the transonic regime. Flutter results of transonic codes are compared with those obtained by linear flat plate theory.

Nomenclature

a_h = distance in semi-chord measured from midchord to elastic axis
b,c = semi-chord and full-chord lengths, respectively
C_{lh} = lift coefficient due to plunging
$C_{l\alpha}$ = lift coefficient due to pitching
C_{mh} = moment coefficient due to plunging
$C_{m\alpha}$ = moment coefficient due to pitching
g = structural damping coefficient
h = plunging degree of freedom
I_α = polar moment of inertia about elastic axis
k_b, k_c = reduced frequencies defined as $\omega b/U$ and $\omega c/U$, respectively
k_h, k_α = bending and torsional stiffness coefficients, respectively
m = mass of the airfoil per unit span
q = $\frac{1}{2}\rho U^2$, dynamic pressure
Q_h, Q_α = aerodynamic lifting force and moment, positive in $+h$ and $+\alpha$ directions, respectively
r_α = $(I_\alpha/mb^2)^{1/2}$, radius of gyration about elastic axis
S = airfoil static moment about elastic axis
U = freestream velocity
x_p = distance in semi-chord measured from mid-chord to pitching axis
x_α = S/mb, distance in semi-chord measured from elastic axis to mass center
α = pitching degree of freedom
μ = $m/\pi\rho b^2$, airfoil/air mass density ratio
ρ = freestream air density
ω = flutter frequency
ω_h = $(k_h/m)^{1/2}$, uncoupled plunging frequency
ω_α = $(k_\alpha/I_\alpha)^{1/2}$, uncoupled pitching frequency
ω_r = reference frequency set equal to unity

Received March 15, 1979; revision received Oct. 11, 1979.

Index categories: Aeroelasticity and Hydroelasticity; Nonsteady Aerodynamics; Subsonic and Transonic Flow.

*Professor and Head, School of Aeronautics and Astronautics. Associate Fellow AIAA.

†Graduate Research Assistants, School of Aeronautics and Astronautics. Member AIAA.

‡Principal Scientist, Analysis and Optimization Branch, Structures and Dynamics Division, Flight Dynamics Laboratory. Member AIAA.

Introduction

THE numerical methods for the computation of aerodynamic forces of small-disturbance transonic flows about oscillating airfoils and planar wings have been rapidly developed in recent years. A brief mention of such developments containing 32 references can be found in Ref. 1. It has thus become possible now to employ such developments for aeroelastic applications. A comprehensive state-of-the-art review of the developments in transonic aeroelasticity is given by Ashley.[2]

In Ref. 3, Traci et al. performed a flutter analysis for the NACA 64A006 and NACA 64A410 airfoils based upon the aerodynamic coefficients computed by using the relaxation programs STRANS and UTRANS.[4,5] The aerodynamic coefficients were obtained for the airfoils pitching about the leading edge. The moment coefficients were then transformed from the leading edge to the elastic axis for flutter analysis. Standard *U-g* method[6] was used. Flutter results were obtained for a NACA 64A006 airfoil with plunging and pitching degrees of freedom. For the case studied, it was demonstrated that the curve for the flutter velocity dropped in the region near $M = 0.85$. The restricted aerodynamic data did not permit an in-depth examination of the NACA 64A410 airfoil. The effects of mean angle of attack and wind tunnel wall interference on the flutter parameters for the NACA 64A006 airfoil were also examined for a limited case.

An additional degree of freedom of aileron oscillation was also examined. Due to the rather restricted reduced frequency range of their aerodynamic data, the true flutter velocity was not obtainable because an aileron dominated mode was fluttering at a frequency out of the data range.

Ballhaus and Goorjian[7] proposed to use the time-integration and the indicial approaches for the aeroelastic response problems. They performed an aeroelastic response analysis for a NACA 64A006 airfoil with a single pitching degree of freedom. The responses were computed by using the computer program LTRAN2 for unsteady transonic flow coupled with an integration procedure for the simple differential equation of motion for the airfoil.

As a visiting scientist at the Air Force Flight Dynamics Laboratory, Rizzetta completed three reports.[8-10]

In Ref. 8, Rizzetta performed a flutter analysis for a NACA 64A010 airfoil with two degrees of freedom, plunge and pitch. The steady and unsteady flows were computed by using the relaxation programs STRANS and UTRANS,[3] respectively. Flutter velocities and frequencies were computed for two Mach numbers (0.72 and 0.80) and two angles of attack (0 and 1 deg).

In Ref. 9, Rizzetta performed a comparative study of the relaxation programs STRANS2 and UTRANS2[4,5] and the time-integration program LTRAN2[11] for calculating the steady and unsteady aerodynamic pressures for a NACA 64A010 airfoil. Mach numbers considered were 0.72 and 0.82. The pitching amplitude was $\alpha = 1$ deg and the reduced frequencies k_c were 0.05 and 0.2. A mean angle of attack of 1 deg was also considered for $M = 0.72$, $\alpha = 0.5$ deg, and $k_c = 0.05$. The agreement between the two methods was good except for the unsteady results at $M = 0.82$ with the presence of shock. In that case, the peak lift value obtained from the time-integration method was approximately 50% higher than that from the harmonic analysis.

In Ref. 10, Rizzetta performed an aeroelastic response study of a NACA 64A010 airfoil by integrating the LTRAN2 program and the structural equations of motion. The study included a single degree of freedom case of pitching and a three degrees of freedom case of pitching, plunging, and aileron pitching. The two degrees of freedom case and the single plunging degree of freedom case were not included. Mach numbers considered were 0.72 and 0.82. Results were shown as plots of nondimensional pitching displacement (and moment), plunging displacement (and lift), and aileron displacement (and moment) vs time for various airfoil/air mass density ratios.

A wind tunnel study was conducted by Farmer and Hanson[12] to investigate flutter characteristics of two dynamically similar wings: one with a supercritical airfoil and the other with a conventional airfoil. The two wings had the same planform, same maximum thickness/chord ratio, and nearly identical stiffness and mass distributions. The flutter boundaries of the two wings were measured and compared with those obtained from a subsonic lifting surface theory. It was found that the theory and experiment correspond well up to $M = 0.85$. Analytical results did not indicate the large transonic dip found experimentally for both wings. It was also found that the flutter boundaries of the two wings were nearly identical up to $M = 0.9$, after which the supercritical wing experienced a much more pronounced transonic dip.

McGrew et al.[13] carried out flutter analyses of supercritical wings in transonic flows. They analyzed two cases, a TF-8A flutter model and the YC-15II prototype aircraft. It was demonstrated that supercritical wings exhibit significantly lower flutter speeds than a conventional wing of equal size and rigidities. This agrees with conclusions made in Ref. 12. Also the conclusions of Ref. 13 on the importance of shock effects reinforce those arrived at by Ashley.[2]

Ashley[2] discussed in detail the role of shocks in the "subtransonic" flutter phenomenon. A semi-quantitative investigation was carried out on the influence of partial-chord transonic shocks on flutter of "typical section" wing models. Flutter characteristics for one (pitch) and two (pitch and plunge) degree of freedom systems were obtained. The effects of airfoil/air mass density ratio, position of mass center, flexure/torsion frequency ratio, and Mach number on the flutter velocity were studied. The general trends are similar to those found in this paper. One of the important features in Ref. 2 is the procedure to consider the shock movement during the flutter analysis.

In this paper, flutter analysis was performed for a NACA 64A006 airfoil with pitching and plunging degrees of freedom at various transonic Mach numbers. Two parallel sets of aerodynamic coefficients were obtained by using both the relaxation method (STRANS2 and UTRANS2) and the indicial method (LTRAN2). It is noted that in LTRAN2 a low frequency approximation is used.

The unsteady aerodynamic coefficients C_{lh}, $C_{l\alpha}$, C_{mh}, and $C_{m\alpha}$, required for flutter analyses, were obtained by pitching the airfoil about the quarter chord. It is noted here that the original version of LTRAN2 has provision to compute only moments about the midchord. For the present analyses changes were made in LTRAN2 to compute the moments about the quarter chord.

The Mach numbers considered were 0.7, 0.8, 0.85, 0.8625, and 0.87, respectively. For each Mach number, flutter velocities and the corresponding reduced frequencies were obtained by varying the airfoil/air mass density ratio μ, plunge/pitch frequency ratio ω_h/ω_α, location of mass center x_α, and location of elastic axis a_h. The effect of each parameter on the trend of each curve of flutter speed is discussed in detail. The effect of Mach number on the flutter speed is also studied.

For all the examples studied, the two sets of curves for flutter velocity, one based upon the aerodynamic coefficients computed by using LTRAN2 and the other upon those computed by using UTRANS2 are compared and discussed. Present results are also compared with those obtained by linear flat plate theory.

Aeroelastic Equations of Motion

The parameters and sign conventions for a typical airfoil oscillating with pitching and plunging degrees of freedom are defined in Fig. 1. The system is similar to that discussed in Sec. 9-2 of Ref. 6.

It is assumed that the airfoil is rigid and the amplitudes of oscillation are small. It is also assumed that the principle of superposition for airloads is valid even in the presence of shock. Validity of this assumption was shown by preliminary wind tunnel results obtained by S. Davis of NASA Ames for NACA 64A010 airfoils oscillating with zero mean angle of attack.[14] All cases studied here are with zero angle of attack.

Considering the inertia forces, elastic forces, and aerodynamic forces, the equations of motion are

$$Q_h = m\ddot{h} + S\ddot{\alpha} + k_h h$$

$$Q_\alpha = S\ddot{h} + I_\alpha \ddot{\alpha} + k_\alpha \alpha \tag{1}$$

or

$$\ddot{\xi} + x_\alpha \ddot{\alpha} + \xi \omega_h^2 = Q_h/mb$$

$$x_\alpha \ddot{\xi} + r_\alpha^2 \ddot{\alpha} + r_\alpha^2 \omega_\alpha^2 \alpha = Q_\alpha/mb^2 \tag{2}$$

where $\xi = h/b$, $\omega_h = (k_h/m)^{1/2}$, $x_\alpha = S/mb$, $\omega_\alpha = (k_\alpha/I_\alpha)^{1/2}$, and $r_\alpha = (I_\alpha/mb^2)^{1/2}$.

Structural damping can be introduced into Eqs. (2) by replacing ω_h^2 and ω_α^2 by $\omega_h^2(1+g_h)$ and $\omega_\alpha^2(1+g_\alpha)$, respectively. The damping coefficients g_h and g_α correspond to plunging and pitching modes, respectively. It is further assumed that g_h and g_α are small and of the same order.

Assuming harmonic oscillations with flutter frequency ω and expressing the aerodynamic forces Q_h and Q_α in terms of aerodynamic coefficients C_{lh}, $C_{l\alpha}$, C_{mh}, and $C_{m\alpha}$, Eqs. (2)

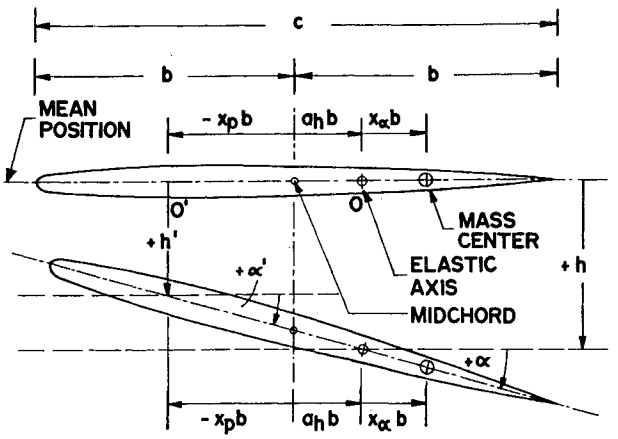

Fig. 1 Definition of parameters for two degrees of freedom aeroelastic system.

yield the final eigenvalue equations for flutter analysis as

$$\{\mu k_b^2[M]-[A]\}\begin{Bmatrix}\xi_0\\ \alpha_0\end{Bmatrix}=\lambda[K]\begin{Bmatrix}\xi_0\\ \alpha_0\end{Bmatrix} \tag{3}$$

where ξ_0 and α_0 are the nondimensional amplitudes in plunge and pitch oscillations, respectively; $\mu=m/\pi\rho b^2$, the airfoil/air mass density ratio; $k_b=\omega b/U$, the reduced frequency. The matrices $[M]$, $[A]$, and $[K]$ are defined as

$$[M]=\begin{bmatrix}1 & x_\alpha\\ x_\alpha & r_\alpha^2\end{bmatrix} \tag{4a}$$

$$[A]=\frac{1}{\pi}\begin{bmatrix}C_{lh}/2 & C_{l\alpha}\\ -C_{mh} & -2C_{m\alpha}\end{bmatrix} \tag{4b}$$

$$[K]=\begin{bmatrix}(\omega_h/\omega_r)^2 & 0\\ 0 & r_\alpha^2(\omega_\alpha/\omega_r)^2\end{bmatrix} \tag{4c}$$

The eigenvalue λ is a complex number defined as

$$\lambda=\mu(1+ig)\omega_r^2 b^2/U^2 \tag{5}$$

where $g(=g_h=g_\alpha)$ is the structural damping coefficient which is assumed to be small and of the same order for both plunging and pitching modes. The flutter solution is obtained when g is found to be zero.[6] In the transonic flutter analysis, to compute the aerodynamic coefficients for Eq. (4b) comprises the essential task.

Transformation of Aerodynamic Coefficients

In obtaining the aerodynamic coefficients, it is a common practice to pitch the airfoil about the elastic axis so that such coefficients can be directly used to compute the aerodynamic matrix $[A]$ in Eq. (4b). But in some situations that may not be the case. For example, the position of the elastic axis is considered to be a variable in this paper so that its effect on flutter characteristics can be studied. Thus the aerodynamic coefficients originally obtained with reference to a pitching axis must be transformed to those with reference to the elastic axis for aeroelastic analysis. The transformation relations can be derived by using the principle of superposition of airloads.

Let it be assumed that the aerodynamic coefficients C'_{lh}, $C'_{l\alpha}$, C'_{mh}, and $C'_{m\alpha}$ for point 0′ (see Fig. 1) due to pitching about 0′ have been obtained. It is desired to transform these coefficients to be C_{lh}, $C_{l\alpha}$, C_{mh}, and $C_{m\alpha}$ for another pitching axis (elastic axis) 0.

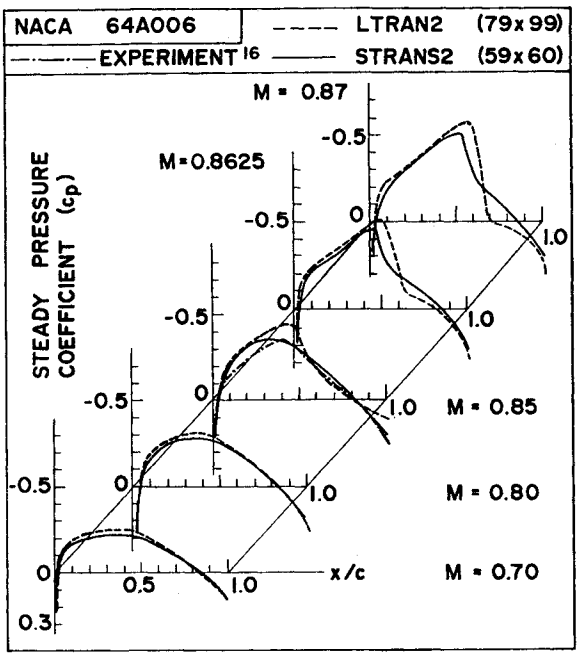

Fig. 2 Distributions of steady pressure coefficients at $M=0.7$, 0.8, 0.85, 0.8625, and 0.87, respectively.

Assuming rigid airfoil and small amplitude of oscillations, the transformation relationships may be written as

$$\begin{aligned}C_{lh}&=C'_{lh}\\ C_{l\alpha}&=C'_{l\alpha}-(sC'_{lh})\\ C_{mh}&=C'_{mh}+sC'_{lh}\\ C_{m\alpha}&=C'_{m\alpha}+sC'_{l\alpha}-(sC'_{mh})-(s^2C'_{lh})\end{aligned} \tag{6}$$

where $s=(a_h-x_p)/2$. The three terms in the parentheses are relatively small when compared with the other terms. If they are neglected, Eqs. (6) are in the form as those given previously by Traci et al.[3]

Results of Aerodynamic Computations

A NACA 64A006 airfoil was chosen for the present analysis. The equations for the configuration were based on those given in Ref. 15.

The four aerodynamic coefficients C_{lh}, $C_{l\alpha}$, C_{mh}, and $C_{m\alpha}$ were computed by using both the relaxation programs STRANS2 and UTRANS2[3-5] and the indicial and time-integration program LTRAN2.[7,11] The airfoil was assumed to pitch about the 1/4 chord axis. The results are presented in Tables 1-4 for $M=0.8$, 0.85, 0.8625, and 0.87, respectively. The finite difference meshes used are also given in the respective tables. In each table, only five or six different values of low reduced frequencies with selected intervals were considered. In the search for flutter solutions, it is necessary that the aerodynamic coefficients be a function of reduced frequency. Such functions were obtained by using the Lagrange interpolation formula based on those known values given in Tables 1-4.

It is difficult to draw conclusions consistent among all tables on the comparison of the two sets of results. However, the agreements in real parts are, in general, better than those in imaginary parts. The agreements in lifting coefficients are, in general, better than those in moment coefficients. The comparisons in higher Mach numbers are not as good when compared to those in the lower Mach numbers. This may be attributed to the difference in the strength and position of the shocks predicted by the two computer programs. It may also

Table 1 Aerodynamic coefficients for NACA 64A006 airfoil and linear flat plate pitching at the quarter-chord at $M=0.80$

		Reduced frequency, k_c											
		0.0		0.05		0.10		0.15		0.20		0.22	
	Method[a]	Real	Imag.	Real	Imag.	Real	Imag.	Real	Imag.	Real	Imag.	Real	Imag.
C_{lh}	1	0.0	0.0	0.070	0.520	0.264	0.978	0.534	1.331	0.821	1.569	0.929	1.636
	2	0.0	0.0	0.115	0.540	0.253	0.893	0.518	1.154	0.749	1.326	0.797	1.235
	3	0.0	0.0	0.094	0.451	0.239	0.786	0.374	1.051	0.488	1.277	0.528	1.360
$C_{l\alpha}$	1	10.620	0.0	10.400	−1.406	9.778	−2.637	8.874	−3.557	7.846	−4.105	7.437	−4.221
	2	11.291	0.0	10.029	−2.028	8.651	−2.853	7.319	−3.063	6.247	−2.830	5.844	−2.683
	3	10.472	0.0	9.075	−1.654	7.988	−2.001	7.219	−1.977	6.672	−1.821	6.498	−1.742
C_{mh}	1	0.0	0.0	−0.000	−0.017	−0.001	−0.034	−0.003	−0.051	−0.005	−0.068	−0.005	−0.075
	2	0.0	0.0	0.002	−0.016	0.011	−0.028	0.019	−0.049	0.026	−0.072	0.020	−0.075
	3	0.0	0.0	0.003	−0.001	0.013	−0.004	0.026	−0.010	0.043	−0.019	0.051	−0.023
$C_{m\alpha}$	1	−0.342	0.0	−0.342	0.006	−0.342	0.011	−0.341	0.017	−0.341	0.022	−0.341	0.025
	2	−0.283	0.0	−0.279	−0.076	−0.292	−0.148	−0.306	−0.204	−0.316	−0.251	−0.319	−0.262
	3	0.0	0.0	−0.014	−0.096	−0.038	−0.193	−0.061	−0.279	−0.083	−0.358	−0.091	−0.389

[a]Method 1: Indicial method with 79×99 grid, NACA 64A006 airfoil. Method 2: Relaxation method with 59×60 grid, NACA 64A006 airfoil. Method 3: Kernel function method, linear flat plate.

Table 2 Aerodynamic coefficients for NACA 64A006 airfoil and linear flat plate pitching at the quarter-chord at $M=0.85$

		Reduced frequency, k_c											
		0.0		0.05		0.10		0.15		0.18		0.25	
	Method[a]	Real	Imag.	Real	Imag.	Real	Imag.	Real	Imag.	Real	Imag.	Real	Imag.
C_{lh}	1	0.0	0.0	0.136	0.666	0.492	1.180	0.938	1.470	1.187	1.525	1.570	1.480
	2	0.0	0.0	0.163	0.626	0.480	0.962	0.783	1.148	0.832	1.039	...	...
	3	0.0	0.0	0.125	0.490	0.300	0.826	0.453	1.082	0.532	1.215	0.682	1.492
$C_{l\alpha}$	1	13.860	0.0	13.310	−2.720	11.820	−4.920	9.770	−6.250	8.474	−6.596	5.900	−6.280
	2	14.653	0.0	11.803	−3.701	9.160	−4.491	7.223	−4.076	5.804	−3.689	...	...
	3	11.927	0.0	9.874	−2.251	8.422	−2.595	7.472	−2.499	7.059	−2.374	6.384	−2.030
C_{mh}	1	0.0	0.0	−0.001	−0.034	−0.005	−0.068	−0.012	−0.102	−0.018	−0.122	−0.037	−0.168
	2	0.0	0.0	0.004	−0.026	0.009	−0.054	0.013	−0.089	0.002	−0.096	...	...
	3	0.0	0.0	0.004	−0.001	0.016	−0.007	0.033	−0.018	−0.044	−0.025	0.074	−0.048
$C_{m\alpha}$	1	−0.676	0.0	−0.676	0.021	−0.677	0.053	−0.677	0.082	−0.677	0.101	−0.673	0.148
	2	−0.530	0.0	−0.501	−0.071	−0.510	−0.147	−0.514	−0.210	−0.498	−0.180	...	...
	3	0.0	0.0	−0.026	−0.127	−0.070	−0.243	−0.109	−0.339	−0.132	−0.393	−0.182	−0.511

[a]Method 1: Indicial method with 79×99 grid, NACA 64A006 airfoil. Method 2: Relaxation method with 59×60 grid, NACA 64A006 airfoil. Method 3: Kernel function method, linear flat plate.

be attributed to the differences in aerodynamic equation, numerical method, and mesh, etc. However, the emphasis in this study is to compare the flutter solutions resulted from the two sets of aerodynamic coefficients.

Figure 2 shows the distributions of steady pressure coefficients across the airfoil for $M=0.7$, 0.8, 0.85, 0.8625, and 0.87, respectively. In both programs (STRANS2 and LTRAN2) the steady solutions are based upon the relaxation method. The differences between the two sets of pressure curves are predominantly due to the difference in mesh size. Tijdeman's experimental results for $M=0.85$ are also shown in Fig. 2 for comparison.[16]

It is of interest to compare the aerodynamic coefficients obtained by using the present two transonic codes with those obtained by using the linear flat plate theory. Many methods are available (see Chap. 6 of Ref. 6) to compute the aerodynamic coefficients of an oscillating airfoil in two-dimensional subsonic flow. In this study, the kernel function method (Sec. 6-4, Ref. 6) was employed to obtain the aerodynamic coefficients. Dr. S.R. Bland of NASA Langley provided a computer program to obtain the aerodynamic coefficients by this method. In this program the kernel of the two-dimensional Poisson equation (Eq. 6-111 of Ref. 6) is obtained by the Laguerre-Gauss quadrature method. The aerodynamic coefficients obtained by the transonic codes compared well with those obtained by kernel function method at $M=0.7$ (see Ref. 1). The aerodynamic coefficients obtained by kernel function method for $M=0.8$, 0.85, 0.8625, and 0.87 are shown in Tables 1-4 as a set reference.

Results of Flutter Analysis

As suggested by Bland, flutter analysis was first performed for a flat plate plunging and pitching about the quarter chord axis at a subsonic speed ($M=0.7$) based on the relaxation and indicial transonic codes and the linear flat plate theory. Comparison of the flutter results indicated that the two transonic codes agree with the linear flat plate theory at $M=0.7$.

Flutter analysis was then performed for a NACA 64A006 airfoil with plunging and pitching degrees of freedom. The effects of four parameters were considered: airfoil/air mass density ratio μ, position of the mass center x_α, position of the elastic axis a_h, and the plunge/pitch frequency ratio ω_h/ω_α. In all cases, the radius of gyration r_α and the reference frequency ω_r were assumed to be 0.5 and 1.0 respectively.

Table 3 Aerodynamic coefficients for NACA 64A006 airfoil and linear flat plate pitching at the quarter-chord at $M=0.8625$

		Reduced frequency, k_c									
		0.0		0.05		0.10		0.15		0.20	
	Method[a]	Real	Imag.	Real	Imag.	Real	Imag.	Real	Imag.	Real	Imag.
C_{lh}	1	0.0	0.0	0.159	0.730	0.580	1.288	1.123	1.569	1.615	1.565
	2	0.0	0.0	0.220	0.591	0.504	0.866	0.730	0.994	...	...
	3	0.0	0.0	0.135	0.502	0.320	0.836	0.478	1.088	0.607	1.301
$C_{l\alpha}$	1	15.204	0.0	14.589	−3.169	12.881	−5.798	10.457	−7.487	7.825	−8.075
	2	15.482	0.0	11.958	−4.091	9.178	−4.756	7.018	−4.387	...	...
	3	12.416	0.0	10.110	−2.459	8.534	−2.788	7.530	−2.662	6.863	−2.419
C_{mh}	1	0.0	0.0	−0.013	−0.076	−0.047	−0.141	−0.096	−0.188	−0.149	−0.214
	2	0.0	0.0	−0.009	−0.049	−0.020	−0.085	−0.035	−0.118	...	...
	3	0.0	0.0	0.005	−0.002	0.018	−0.009	0.035	−0.020	0.055	−0.036
$C_{m\alpha}$	1	−1.558	0.0	−1.520	0.250	−1.412	0.471	−1.253	0.640	−1.070	0.746
	2	−1.184	0.0	−0.977	0.119	−0.899	0.085	−0.821	0.054	...	...
	3	0.0	0.0	−0.032	−0.138	−0.083	−0.259	−0.129	−0.359	−0.171	−0.449

[a]Method 1: Indicial method with 79×99 Grid, NACA 64A006 airfoil. Method 2: Relaxation method with 59×60 Grid, NACA 64A006 airfoil. Method 3: Kernel function method, linear flat plate.

Table 4 Aerodynamic coefficients for NACA 64A006 airfoil and linear flat plate pitching at the quarter-chord at $M=0.87$

		Reduced frequency, k_c									
		0.0		0.05		0.10		0.15		0.20	
	Method[a]	Real	Imag.	Real	Imag.	Real	Imag.	Real	Imag.	Real	Imag.
C_{lh}	1	0.0	0.0	0.191	0.760	0.693	1.376	1.324	1.609	1.861	1.499
	2	0.0	0.0	0.219	0.554	0.486	0.798	0.657	0.914	...	...
	3	0.0	0.0	0.143	0.509	0.333	0.842	0.494	1.092	0.624	1.302
$C_{l\alpha}$	1	16.691	0.0	15.191	−3.817	13.756	−6.930	10.727	−8.824	7.494	−9.305
	2	14.732	0.0	11.082	−3.963	8.393	−4.368	6.469	−3.980	...	...
	3	12.743	0.0	10.260	−2.599	8.602	−2.914	7.562	−2.767	6.879	−2.509
C_{mh}	1	0.0	0.0	−0.031	−0.125	−0.114	−0.217	−0.220	−0.254	−0.317	−0.235
	2	0.0	0.0	−0.015	−0.056	−0.035	−0.091	−0.053	−0.119	...	...
	3	0.0	0.0	0.005	−0.002	0.019	−0.010	0.036	−0.023	0.056	−0.040
$C_{m\alpha}$	1	−2.624	0.0	−2.503	0.621	−2.168	1.137	−1.692	1.469	−1.175	1.586
	2	−1.396	0.0	−1.119	0.224	−0.952	0.203	−0.845	0.177	...	...
	3	0.0	0.0	−0.036	−0.145	−0.092	−0.270	−0.142	−0.372	−0.189	−0.463

[a]Method 1: Indicial method with 79×99 grid, NACA 64A006 airfoil. Method 2: Relaxation method with 59×60 grid, NACA 64A006 airfoil. Method 3: Kernel function method, linear flat plate.

Effect of Position of Mass Center x_α

The NACA 64A006 airfoil was assumed to pitch about the 1/4 chord axis. The airfoil/air mass density ratio was assumed as 100.

Curves for flutter speed and the corresponding reduced frequency vs the location of mass center x_α were obtained for three different values of plunge/pitch frequency ratio. The mass center was moved from 1/4 chord to 1/2 chord. The curves are shown in Figs. 3 and 4 for $M=0.8$ and 0.87, respectively. Similar curves were also obtained for $M=0.85$ and 0.8625, respectively, but are not shown here.

At all Mach numbers the same general trend is observed. The flutter speed decreases as the mass center moves from the elastic (pitch) axis toward the midchord. It increases very sharply as the mass center approaches the pitching axis. The curves drop as ω_h/ω_α increases. The curves for the reduced frequency demonstrate a behavior opposite to that of the flutter curves.

For $M=0.8$ and 0.85, the set of flutter speed curves obtained by the indicial method and the set by the relaxation method are in excellent agreement. As Mach number increases, the two sets of curves shift gradually toward the right but still maintain the same trend. The former set shifts faster than the latter. Thus the two sets become quite apart at $M=0.87$ where a meaningful comparison in flutter speed between the two methods is virtually impossible when $x_\alpha<0.4$.

The difference between the two sets of flutter speed curves at higher Mach number is, of course, reflected in Tables 3 and 4 for aerodynamic coefficients. Such difference may be attributed to the lack of agreement in the position and strength of the shocks computed by the two methods. It may also be attributed to the differences in aerodynamic equation, numerical procedure, mesh, etc.

Effect of Airfoil/Air Mass Density Ratio μ

The NACA 64A006 airfoil was assumed to pitch about the quarter chord axis. The mass center was assumed to be at $x_\alpha b$ aft the elastic (pitch) axis where $x_\alpha=0.25$ and 0.5 for $M=0.8$ and 0.87, respectively. As explained earlier in connection with Fig. 4, x_α must be somewhat greater than 0.4 for $M=0.87$ in order to obtain a meaningful comparison in flutter speed between the two methods.

Curves for flutter speed and the corresponding reduced frequency vs the airfoil/air mass density ratio μ were obtained for various frequency ratios. The μ value was varied from 25 to 300. The curves are shown in Figs. 5 and 6 for $M=0.8$ and 0.87, respectively. Similar curves were also obtained for $M=0.85$ and 0.8625, respectively, but are not shown here.

At all the Mach numbers the same general trend is observed. The flutter speed increases steadily with μ. The curves become less steep for higher frequency ratios. For each μ value, the flutter speeds are lower for higher frequency ratios.

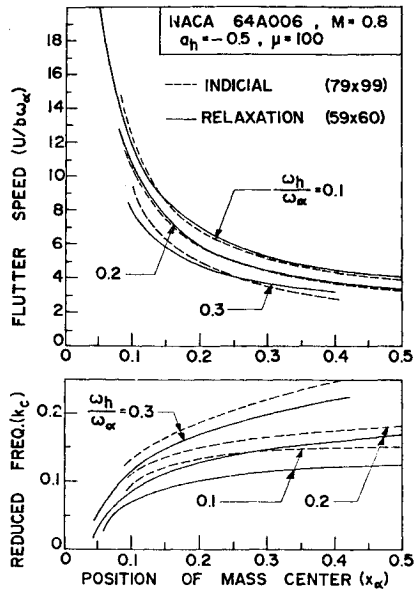

Fig. 3 Effect of position of mass center on flutter speed for various frequency ratios at $M=0.8$.

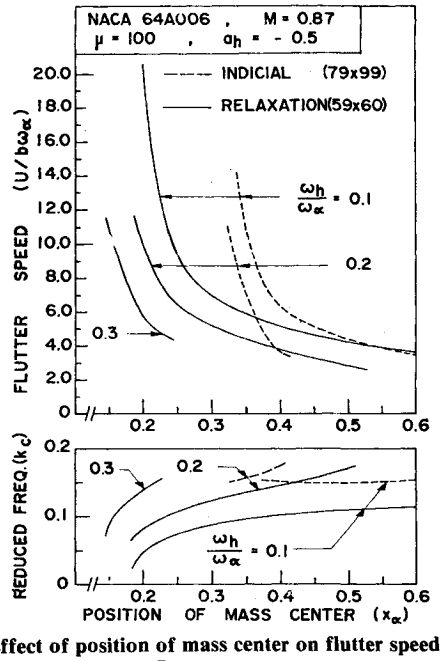

Fig. 4 Effect of position of mass center on flutter speed for various frequency ratios at $M=0.87$.

The reduced frequency k_c increases as μ decreases and k_c curves are higher for higher frequency ratios. It becomes difficult to obtain flutter results for both lower μ values and higher frequency ratios since k_c goes out of the valid range (say, $k_c<0.25$) of the present methods.

The two sets of curves, one by the indicial method and the other by the relaxation method are, in general, in good agreement. The level of agreement becomes lower for higher Mach numbers. This may be attributed to the diffeence in the position and strength of the shocks predicted by the two methods plus other differences, such as aerodynamic equation, numerical procedure, mesh, etc.

Effect of Position of Elastic (Pitch) Axis a_h

Since all the aerodynamic coefficients were obtained by pitching the airfoil about the quarter chord axis ($a_h=-0.5$), it was necessary to use the transformation Eqs. (6) when a_h was varied. The mass density ratio was fixed at 100. The mass

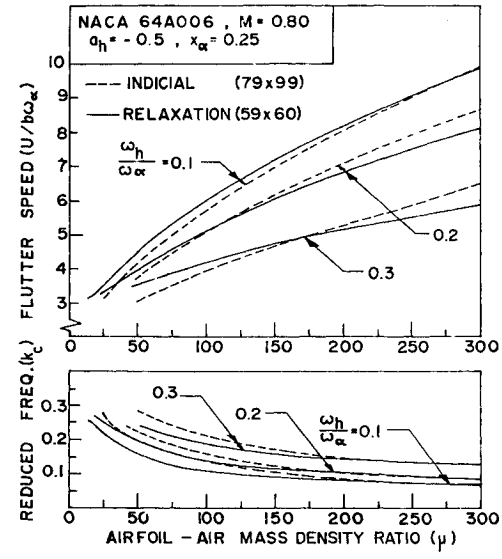

Fig. 5 Effect of mass density ratio on flutter speed for various frequency ratios at $M=0.8$.

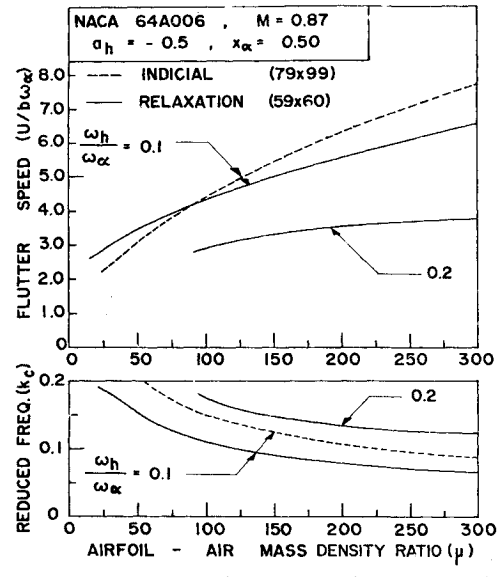

Fig. 6 Effect of mass density ratio on flutter speed for various frequency ratios at $M=0.87$.

center was fixed at 3/8 chord for $M=0.8$. As explained earlier in connection with Fig. 4, the mass center was moved aft for higher M in order to obtain meaningful comparison in flutter speed between the two methods.

Curves for flutter speed and the corresponding reduced frequency vs a_h were obtained for various frequency ratios. The elastic (pitch) axis was moved from 20 to 45% chord. The curves are shown in Fig. 7 for $M=0.8$. Similar curves were also obtained for $M=0.85$, 0.8625, and 0.87, respectively, but are not shown here.

At all Mach numbers the same general trend is observed. The flutter speed increases as the elastic axis moves toward the midchord. Such increasing trend becomes less obvious for lower frequency ratios. The two methods compare well.

When the mass center coincides with the elastic axis ($x_\alpha=0$), the plunge and pitch motions become uncoupled in the mass matrix in Eq. (4a). If C_{mh} in Eq. (4b) also vanishes it can be shown that one of the two eigenvalues becomes independent of the frequency ratio. In this study, C_{mh} are very small as compared with the other three coefficients in Tables 1-4. Thus the flutter curves may intersect when x_α is somewhere close to zero. This turns out to be the case in Fig. 7.

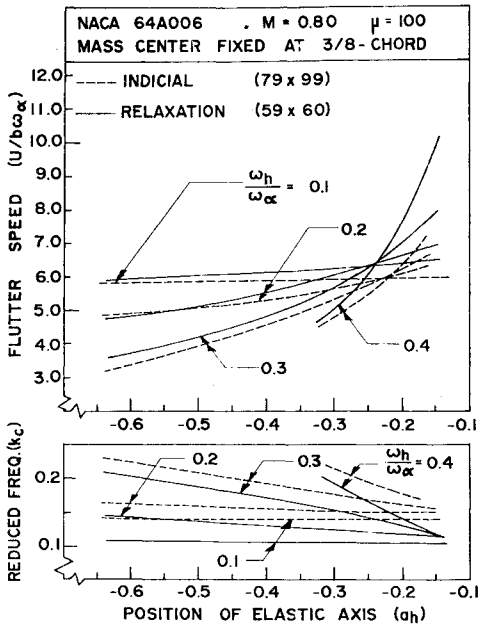

Fig. 7 Effect of position of elastic axis on flutter speed for various frequency ratios at $M = 0.8$.

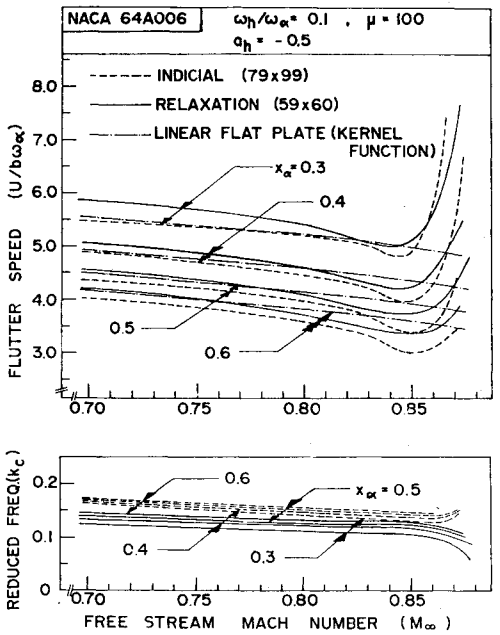

Fig. 9 Effect of Mach number on flutter speed for various mass center positions.

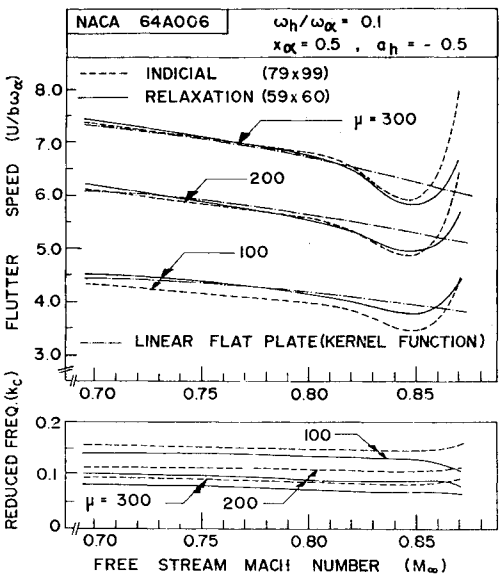

Fig. 8 Effect of Mach number on flutter speed for various mass density ratios.

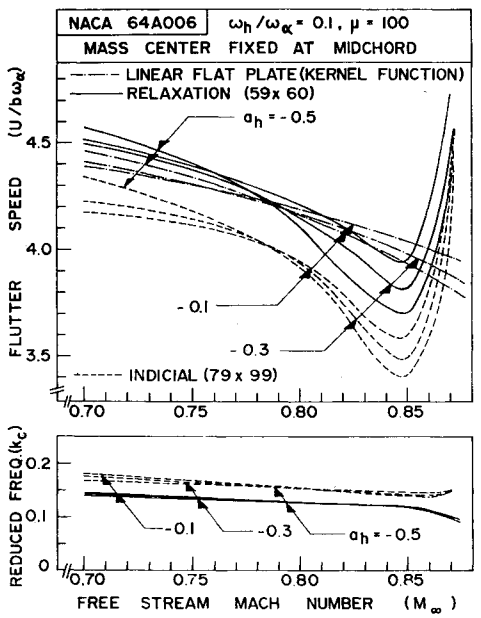

Fig. 10 Effect of Mach number on flutter speed for various elastic axis positions.

Effect of Mach Number M

Curves for flutter speed and the corresponding reduced frequency vs the freestream Mach number were obtained for various values of aeroelastic parameters. The freestream Mach numbers considered for both methods were 0.7, 0.8, 0.85, 0.8625, and 0.87, respectively. Additional flutter results were also computed at Mach numbers of 0.75 and 0.825 based on the indicial method.

Figure 8 shows the curves for flutter speed and the corresponding reduced frequency vs freestream Mach number for three different values of airfoil/air mass density ratio ($\mu = 100$, 200, and 300). The values for a_h, x_α, and ω_h/ω_α were assumed as -0.5, 0.5, and 0.1, respectively.

The interesting "transonic dip" phenomenon found previously (see, for example, Ref. 12) is seen in Fig. 8. Such dip is more pronounced for higher μ values. The two methods agree well except at the high Mach number region such as $M = 0.87$. Such discrepancy has been observed and explained earlier in connection with Figs. 4 and 6.

A set of curves obtained by the linear flat plate theory is also shown in Fig. 8. The curves agree well with those obtained by the two transonic codes at lower Mach numbers. As expected, however, the linear flat plate theory fails to predict the transonic dip phenomenon.

Figure 9 shows the curves for the flutter speed and the corresponding reduced frequency vs freestream Mach number for various positions of mass center ($x_\alpha = 0.3$, 0.4, 0.5, and 0.6, respectively). The values for a_h, μ, and ω_h/ω_α were assumed as -0.5, 100.0, and 0.1, respectively.

The transonic dip phenomenon is again observed in Fig. 9. The dip phenomenon is more pronounced as the mass center moves toward the elastic axis. The two methods agree well. Curves obtained by linear flat plate theory are also plotted in Fig. 9. These curves do not show the transonic dip phenomenon.

Figure 10 shows the curves for the flutter speed and the corresponding reduced frequency vs freestream Mach number

for various positions of elastic axis ($a_h = -0.1$, -0.3, and -0.5, respectively). The mass center is fixed at midchord and the values for μ and ω_h/ω_α were assumed as 100.0 and 0.1, respectively.

The flutter curves in Fig. 10 again illustrate the transonic dip phenomenon. Both methods show similar trends. It can be seen that at lower Mach numbers ($M<0.77$) the flutter speed increases as the elastic axis moves away from the midchord toward the leading edge. On the other hand, for higher Mach numbers ($M>0.77$) an opposite behavior is observed.

Flutter results obtained by linear flat plate theory are also shown in Fig. 10. The flutter speeds continuously decrease with the increase of Mach number and do not present the transonic dip phenomenon.

Conclusion

1) In the computation of Table 3, the indicial method took approximately 2.4 h of computer time and the relaxation method took approximately 4.6 h of computer time on a CDC 6500. If the time-integration method is used for the same mesh as the indicial method, approximately 7.0 h are expected.

2) Due to the low frequency approximation used in LTRAN2, the reduced frequencies k_c considered were mostly not higher than about 0.2. Although the low frequency approximation was not used in UTRANS2, convergence could not be obtained at higher k_c. The k_c values considered were never higher than 0.3.

3) The main difficulty in obtaining flutter solutions was in the upper limitation of k_c. In all cases, the search for flutter points was below the k_c values of 0.25 for LTRAN2 and 0.3 for UTRANS2. Due to such limitation, it was impossible to obtain flutter results for $\mu<25$ and $\omega_h/\omega_\alpha>0.4$.

4) The shock position was fixed during the unsteady computations in both the relaxation and the indicial methods. Allowing the shock movement during computation may influence the aerodynamic coefficients to some extent. Both the indicial and relaxation methods employ time linearized aerodynamic theory for unsteady aerodynamic computation. Limited unsteady computations were performed by the time-integration method (LTRAN2) that allowed the shock to move and employed a nonlinear aerodynamic theory. It was found that at $k_c=0.1$, the absolute values of the lift coefficient C_{l_α} obtained by time-integration, indicial, and relaxation methods were, respectively, equal to 10.0, 10.13, and 9.11 for $M=0.8$. The corresponding values for phase angles were -15.0, -15.1, and -18.3 deg. At $M=0.85$, the absolute values of the lift coefficient obtained by time-integration, indicial, and relaxation methods were equal to 12.32, 12.80, and 10.20, respectively. The corresponding values for phase angles were -30.0, -22.6, and -26.1 deg, respectively. However, as M approaches 0.9, the shock movement and the time-linearization assumption may become more influential.

5) Improvement in transonic codes to allow for higher values of k_c and M is needed.

6) Future work should include the study of supercritical airfoils. Also, the present methods can be extended to analyze aeroelastic systems with control surfaces.

7) Extension of the present two-dimensional transonic codes to account for the three-dimensional case is needed; with such extension, more practical cases of full three-dimensional wing flutter can be studied.

Acknowledgment

This research was sponsored under AFOSR Grant 78-3523. The research was administered by L.J. Huttsell of the Air Force Wright Aeronautical Laboratories. Advice and help from S.R. Bland of NASA Langley, W.F. Ballhaus and P.M. Goorjian of NASA Ames, are appreciated. The suggestion by H. Ashley to consider higher Mach numbers is appreciated.

References

[1] Yang, T.Y., Striz, A.G., and Guruswamy, P., "Flutter Analysis of Two-Dimensional and Two-Degree-of-Freedom Airfoils in Small-Disturbance Unsteady Transonic Flow," AFFDL-TR-78-202, Dec. 1978.

[2] Ashley, H., "On the Role of Shocks in the 'Sub-Transonic' Flutter Phenomenon," AIAA Paper 79-0765 presented at AIAA/ASME/ASCE/AHS 20th Structures, Structural Dynamics, and Materials Conference, St. Louis, Mo., April 4-6, 1979.

[3] Traci, R.M., Albano, E.D., and Farr, J.L., "Small Disturbance Transonic Flows About Oscillating Airfoils and Planar Wings," AFFDL-TR-75-100, June 1975.

[4] Traci, R.M., Albano, E.D., Farr, J.L., and Cheng, H.K., "Small Disturbance Transonic Flows About Oscillating Airfoils," AFFDL-TR-74-37, June 1974.

[5] Farr, J.L., Traci, R.M., and Albano, E.D., "Computer Programs for Calculating Small Disturbance Transonic Flows About Oscillating Airfoils," AFFDL-TR-74-135, Nov. 1974.

[6] Bisplinghoff, R.L., Ashley, H., and Halfman, R.L., *Aeroelasticity,* Addison-Wesley Publishing Co., Reading, Mass., 1955, Sec. 9-2.

[7] Ballhaus, W.F. and Goorjian, P.M., "Computation of Unsteady Transonic Flows by the Indicial Method," *AIAA Journal,* Vol. 16, Feb. 1978, pp. 117-124.

[8] Rizzetta, D.P., "Transonic Flutter Analysis of a Two-Dimensional Airfoil," AFFDL-TM-75-168-FYS, May 1977.

[9] Rizzetta, D.P., "A Comparative Study of Two Computational Methods for Calculating Unsteady Transonic Flows About Oscillating Airfoils," AFFDL-TR-77-188, Nov. 1977.

[10] Rizzetta, D.P., "The Aeroelastic Analysis of a Two-Dimensional Airfoil in Transonic-Flow," AFFDL-TR-77-126, Dec. 1977 (also *AIAA Journal,* Vol. 17, Jan. 1979, pp. 26-32).

[11] Ballhaus, W.F. and Goorjian, P.M., "Implicit Finite Difference Computations of Unsteady Transonic Flows about Airfoils Including the Treatment of Irregular Shock-Wave Motions," *AIAA Journal,* Vol. 15, Dec. 1977, ppl 1728-1735).

[12] Farmer, M.G. and Hanson, P.W., "Comparison of Supercritical and Conventional Wing Flutter Characteristics," *Proceedings AIAA/ASME/SAE 17th Structures, Structural Dynamics, and Materials Conference,* King of Prussia, Pa., April 1976, pp. 608-611 (also NASA TM X-72837, May 1976).

[13] McGrew, J.A., Giesing, J.P., Pearson, R.M., Zuruddin, K., Schmidt, M.E., and Kalman, T.P., "Supercritical Wing Flutter," AFFDL-TR-78-37, March 1978.

[14] Davis, S. and G. Malcolm, "Experiments in Unsteady Transonic Flow," AIAA Paper 79-0769 presented at AIAA/ASME/ASCE/AHS 20th Structures, Structural Dynamics, and Materials Conference, St. Louis, Mo., April 4-6, 1979.

[15] Olsen, J.J., "AGARD Standard Configurations for Aeroelastic Applications of Transonic Unsteady Aerodynamics, Part III, Candidate Airfoil Data," AFFDL-TM-78-6-FBR, Jan. 1978.

[16] Tijdeman, H., "Investigations of the Transonic Flow Around Oscillating Airfoils," NLR-TR-77090U, National Aerospace Laboratory, The Netherlands, Dec. 1977.